Magic Number Clusters of Serine in the Gas Phase

Anne E. Counterman and David E. Clemmer*

Department of Chemistry, Indiana University, Bloomington, Indiana 47405

Received: April 17, 2001; In Final Form: June 27, 2001

Ion mobility measurements and molecular modeling simulations have been used to examine the conformations of electrosprayed serine clusters. Clusters containing as many as 52 serine amino acid units (and one to four protons) are observed. The distribution of singly charged ions is dominated by a peak corresponding to $[8(Ser)+H]^+$. The measured cross section for this ion is in close agreement with a value that is calculated for tightly packed distorted block geometries that arise from molecular modeling studies of octamers comprising zwitterionic amino acid units. Abundant peaks are observed for $[8(Ser)+2H]^{2+}$, $[16(Ser)+2H]^{2+}$, and $[24(Ser)+3H]^{3+}$ clusters, indicating that the octameric unit is a building block in assembly of larger serine clusters.

Introduction

The ability to resolve specific enantiomers of amino acids is currently receiving considerable attention.[1] Recently, Hodges, Julian, and Beauchamp reported that formation of molecular clusters of serine from electrospray of enantiomeric mixtures involves a spontaneous chiral separation,[2] a possibility that was previously noted by Cooks and co-workers.[3] In this system, the $[8(Ser)+H]^+$ ion appears as a magic number[4] in the mass spectrum.[2,3] The results raise some interesting questions about the structure of $[8(Ser)+H]^+$. Cooks suggested that $[8(Ser)+H]^+$ might form a circular geometry in which individual amino acids have extended configurations and are arranged in a head-to-tail fashion (having a pseudo 8-fold symmetry) -structure 1a, shown in Figure 1.[3] Such a structure could be especially stable if monomer units exist as zwitterions. Beauchamp reported two low-energy compact geometries (structures 1b and 1c) generated from modeling the interactions of eight zwitterionic serines (a net cluster charge of zero).[2,5] These structures arise from interactions of compact serine monomer units that are arranged in either a cubelike configuration or a geometry that appears to contain a hexameric subunit. In this report, we examine the geometry of $[8(Ser)+H]^+$ directly using a combination of ion mobility[6,7] and molecular modeling methods. The results indicate that $[8(Ser)+H]^+$ exists as a tightly packed geometry. Additionally, there is evidence that the stable octamer unit is a building block for higher-order clusters containing 16 and 24 serines. Although the geometries of these larger clusters are not completely understood, it appears that after the initial coalescence of octamer units, larger cluster ions adopt new packing distributions that do not resemble combinations of the proposed best-fit structures for $[8(Ser)+H]^+$.

Studies of atomic and molecular clusters in the gas phase have provided insight into initial steps of nucleation and growth phenomena for several decades.[8] The present studies are possible because of the recent advent of electrospray ionization (ESI)[9] for mass spectrometry, which allows a wide range of noncovalently bound biomolecular clusters to be produced in the gas phase. Such studies may provide clues about the initial steps associated with aggregation, crystallization, and other noncovalent associations.

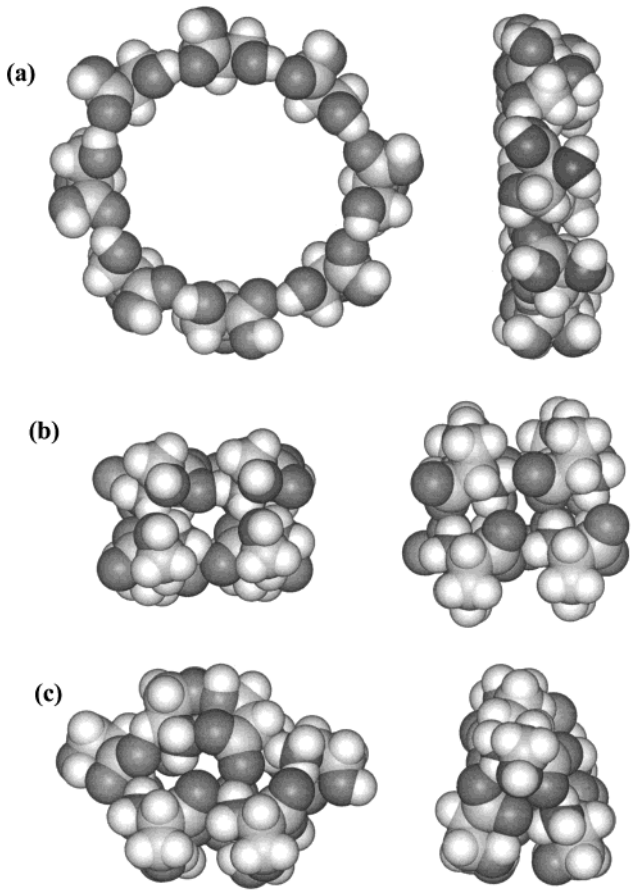

Figure 1. Optimized geometries for Ser_8 constructed based on structures proposed previously. Structure (a) is from ref 3. Structures (b) and (c) are from ref 2. Model (a) is protonated on a single serine unit. Models (b) and (c) are constructed from zwitterionic monomer units; the resulting clusters are neutral. Calculated cross sections for these model geometries are given in Table 1

Experimental Section

Experiments were performed using a hybrid ion mobility/time-of-flight mass spectrometer.[10] Solutions of L-serine (Sigma, used without purification), $\sim 5 \times 10^{-4}$ M to 5×10^{-3} M in

10.1021/jp011421l CCC: $20.00
Published on Web 08/07/2001

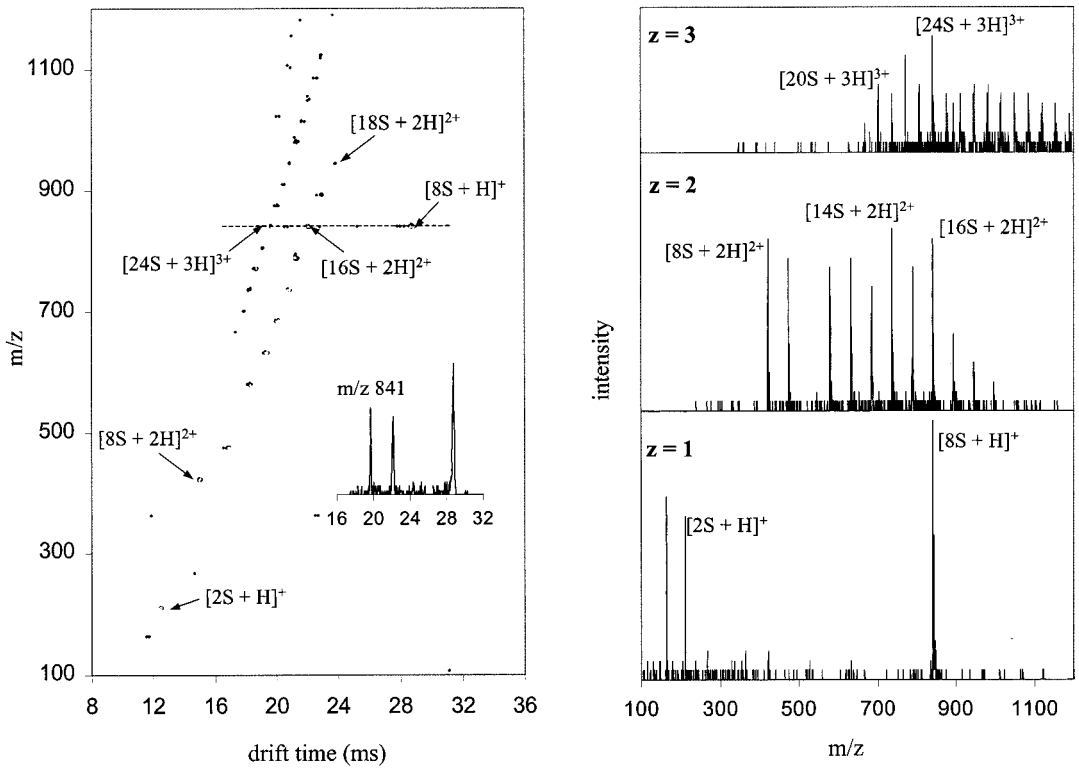

Figure 2. Region of nested drift(flight) times for an electrosprayed solution of L-serine recorded using a buffer gas pressure of 158.62 Torr and an electric field strength of 137.4 V•cm^{-1}. The mass spectra shown on the right were obtained by integrating narrow slices of the two-dimensional data for each charge state family, as delimited by the following lines: for $z = 1$, ($m/z = 41.7 \bullet t_D - 274.1$ and $m/z = 40.7 \bullet t_D - 378.8$); for $z = 2$, ($m/z = 63.1 \bullet t_D - 461.8$ and $m/z = 59.6 \bullet t_D - 567.8$), and for $z = 3$, ($m/z = 87.8 \bullet t_D - 785.3$ and $m/z = 77.4 \bullet t_D - 723.2$), where t_D represents drift time. The inset shows a drift time distribution for the $[8(Ser)+H]^+$, $[16(Ser)+2H]^{2+}$, and $[24(Ser)+3H]^{3+}$ ions obtained by taking a slice across the dataset at *m/z* 841 (indicated by the dashed line).

49:49:2 water:acetonitrile:acetic acid, were electrosprayed[9] into a differentially pumped desolvation region and introduced into a helium-filled drift region. Mobilities (or experimental collision cross sections)[11] are determined by recording the time required for ions to pass through the buffer gas and across the drift tube under the influence of a weak uniform electric field. Compact geometries (with relatively small collision cross sections) have higher mobilities than more open structures.[12] Cluster sizes are determined from time-of-flight data recorded in the mass spectrometer.[10]

Trial geometries were assembled using the InsightII molecular modeling software.[13] A number of 300 K dynamics simulations were carried out. In these studies, a starting geometry is chosen and molecular dynamics simulations are carried out for at least 0.25 ns using the AMBER force field. Simulated annealing studies in which initial geometries (at 300 K) are heated to 400 (or 500) K for 2 ps and then cooled to 300 K were also carried out. Results of the molecular modeling work were monitored by visual inspection of structures at selected timepoints as well as collision cross section calculations (carried out for the twenty-five lowest energy geometries). Cross sections were calculated using the trajectory method developed by Jarrold and co-workers.[14] Trial geometries that are viable candidate structures have calculated cross sections that are within ~2% of experiment.[15,16]

Results and Discussion

A typical two-dimensional plot of the data [a nested drift-(flight) time distribution][10] recorded upon ESI of an L-serine solution is shown in Figure 2. As reported previously for peptide systems,[17] peaks fall into families according to their charge states. Under the experimental conditions employed here, there are four distributions of charge states and cluster sizes: $[2(Ser)+H]^+$ and $[8(Ser)+H]^+$; $[n(Ser)+2H]^{2+}$ ($n = 8$ to 19, where n corresponds to the number of monomer units); $[n(Ser)+3H]^{3+}$ ($n = 20$ to 37); and, $[n(Ser)+4H]^{4+}$ ($n = 32$ to 52). As observed previously,[1,3] the distribution of peaks associated with singly charged ions is dominated by the $[8(Ser)+H]^+$ ion at *m/z* 841.3. Analysis of three datasets yields an average experimental collision cross section for this ion of 191.4 ± 0.2 Å^2. In all datasets, the shape of the $[8(Ser)+H]^+$ peak across the ion mobility dimension can be accurately represented by a calculated distribution for transport of a single geometric structure.[11] This suggests the $[8(Ser)+H]^+$ cluster may favor a single type of geometry that is stable over the ms time scales of these experiment. The resolving power of the present experiment is such that two equally abundant cluster geometries that differed in cross section by as little as ~1% would be resolved.[18]

To obtain insight into the conformation of $[8(Ser)+H]^+$, we have compared the experimental collision cross section with calculated cross sections for trial geometries. We started by examining highly symmetric geometries that were constructed to resemble the extended circular (singly protonated), cubelike (neutral), and hexameric subunit (neutral) configurations (i.e., the structures in Figure 1).[2,3] The calculated cross section for the circular geometry (1a) is 302 Å^2, ~60% larger than the experimental value. Calculated values for the more compact cubelike (1b) and hexameric subunit (1c) geometries are $\Omega =$ 213 and 251 Å^2, respectively, ~11% and 31% larger than experiment.

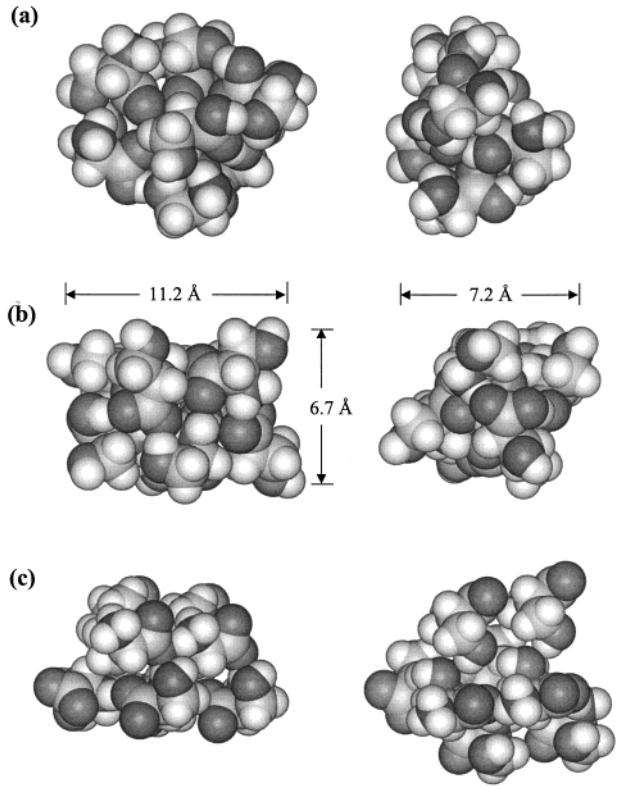

Figure 3. Model geometries for $[8(Ser)+H]^+$. Structure (a) is the lowest energy conformer obtained from a charge-solvated configuration in which only one monomer unit is protonated. Structure (b) is the lowest energy conformer obtained from molecular dynamics simulations of a cluster comprising zwitterionic units. Structure (c) is formed from two unit cells from the crystal structure of L-serine (ref 25). Other slices of the crystal structure that also contain eight monomer units were also examined; the one shown was found to have the lowest calculated collision cross section. Two views of each structure are shown for clarity. Calculated cross sections for these geometries are given in Table 1. See text for details.

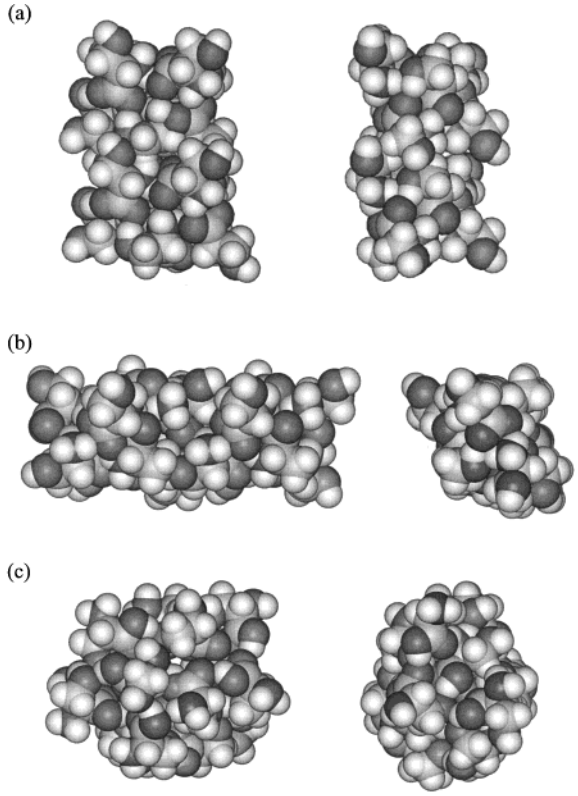

Figure 4. Model geometries for $[16(Ser)+2H]^{2+}$. Geometries (a) and (b) were constructed by stacking the $[8(Ser)+H]^+$ geometry shown in Figure 3b along the 11.2 × 7.2 Å and 6.7 × 7.2 Å interfaces, respectively. Structure (c) is the lowest energy structure obtained from molecular modeling simulations of $[16(Ser)+2H]^{2+}$ in which fourteen serine units are zwitterionic, and the remaining two units contain a protonated N-terminus and uncharged C-terminus. Two views of each structure are shown for clarity. Calculated cross sections for these geometries are given in Table 1. See text for discussion.

To proceed with finding possible candidate geometries, molecular modeling simulations were used to generate trial configurations of the protonated clusters. Several types of starting structures for these simulations were chosen, including the cubelike and hexameric subunit geometries.[2] Simulations were carried out in several ways, including simulated annealing protocols[19] as well as dynamics simulations at 300 K. We began by examining a charge site assignment for $[8(Ser)+H]^+$ in which only one monomer unit is protonated at the N-terminus and the remaining units are uncharged. Simulations yield relatively compact geometries that often adopt low-energy geometries that are somewhat oblate, in which the C-termini of uncharged monomer units solvate the protonation site. Figure 3 shows an example of low-energy geometry (3a) that has one of the most compact structures that we have found. However, the calculated cross section for this structure ($\Omega = 205$ Å^2) is still ~7% larger than experiment. Other low energy structures found for this charge assignment have similar or larger cross sections.

An alternate charge assignment, in which seven serine units are zwitterionic and one is protonated at the N-terminus, yields several types of low-energy structures that have calculated cross sections that are near the experimental value. Figure 3b shows the lowest energy conformation we have found for this charge configuration; the twenty-five lowest energy geometries have an average calculated cross section of 195.3 ± 2.3 Å^2. Within uncertainties, this value is in agreement with experiment. In effect, protonation of one serine disrupts the symmetry of the starting geometry, allowing atoms to pack efficiently in the interior regions. Overall, from the combination of simulations and experiment, it appears that $[8(Ser)+H]^+$ exists in a tightly packed configuration and that the packing appears to favor distorted blocklike geometries. The approximate dimensions of the edges of this block geometry are $\sim 11.2 \pm 0.4 \times 6.7 \pm 0.2 \times 7.2 \pm 0.2$ Å.[20] In some cases, the block appears to twist along the long axis. A common feature associated with these geometries is the packing patterns associated with individual zwitterionic monomers. As expected, the monomeric units are stabilized by formation of salt-bridged structures. Zwitterionic monomer units that are in contact with other zwitterions tend to form salt bridges at each end, and the hydroxyl side chains often interact through hydrogen bonds with deprotonated carboxylic acid endgroups. The single nonzwitterionic serine monomer is typically located at a corner of the blocklike geometry, and the protonated amino terminus appears to be stabilized by interactions with two to three deprotonated carboxylic acid endgroups.

We have also examined possible structures for larger clusters. The data in Figure 2 show that peaks for the $[8(Ser)+2H]^{2+}$ ($\Omega_{expt} = 200$ Å^2), $[16(Ser)+2H]^{2+}$ ($\Omega_{expt} = 294$ Å^2), and $[24(Ser)+3H]^{3+}$ ($\Omega_{expt} = 392$ Å^2) ions, each of which contains a multiple of eight serine units, are often more abundant relative to other cluster sizes in their respective charge state families. For example, the inset mass spectra in Figure 2 shows that clusters containing more than 16 and 24 monomer units in the

TABLE 1: Experimental and Theoretical Collision Cross Sections for $[n(\text{Ser})+z\text{H}]^{z+}$ Clusters

n[a]	z[b]	Ω_{expt}(Å^2)[c]	model geometry[d]	Ω_{calc}(Å^2)[e]
8	1	191.4(0.2)	circle (1a)[f]	301.7
			cubelike (1b)[g]	213.1
			hexameric subunit (1c)[g]	250.9
			charge-solvated (3a)[h]	204.6(5.1)
			zwitterionic (3b)[h]	195.3(2.3)
			crystal structure (3c)[i]	247.9
16	2	294.0(0.6)	forced packing (4a)[j]	367.2
			forced packing (4b)[j]	388.8
			compact ovoid (4c)[h]	304.1(6.3)
24	3	392.4(0.8)		

[a] Number of monomer units contained in the cluster. [b] Net charge state of the cluster. [c] Experimental collision cross sections. Uncertainties given in parentheses correspond to one standard deviation about the mean for replicate measurements. [d] Concise description of the model geometries. Numbers and letters in parentheses indicate the section of each figure in which the geometry is shown. [e] Collision cross section calculated for model geometries using the trajectory method (see ref. 14 for details). For geometries derived from molecular modeling simulations, uncertainties are reported as one standard deviation about the mean value for the twenty-five lowest energy conformers obtained. [f] Singly protonated geometry constructed based on the structure described in ref 3. [g] Neutral geometry constructed based on the structure described in ref 2. [h] Geometry generated by molecular dynamics simulations. See text and ref 13 for more details. [i] An octamer unit extracted from the L-serine crystal structure (ref 25) that has the lowest collision cross section of eight-serine unit slices taken from the crystal packing. [j] Geometries constructed by packing the $[8(\text{Ser})+\text{H}]^+$ blocklike geometry (Figure 3b) along the largest (11.2 × 7.2 Å, 4a) or smallest (6.7 × 7.2 Å, 4b) interface region.

$[n(\text{Ser})+2\text{H}]^{2+}$ and $[n(\text{Ser})+3\text{H}]^{3+}$ families (respectively) have abundances that are lower than the abundance observed for the $n = 16$ and 24 clusters (typically by at least a factor of 2). This suggests that the $[16(\text{Ser})+2\text{H}]^{2+}$ and $[24(\text{Ser})+3\text{H}]^{3+}$ clusters, as well as larger clusters, are assembled from octamer building blocks. It is possible that the $[8(\text{Ser})+\text{H}]^+$ unit may help explain the formation of these larger clusters. For example, addition of two $[8(\text{Ser})+\text{H}]^+$ units to form the $[16(\text{Ser})+2\text{H}]^{2+}$ cluster would explain the decreased relative abundance of doubly protonated clusters containing 17 or more serines. Additionally, loss of serine dimer units from 16(Ser) clusters would explain enhanced abundance of clusters containing even numbers of serines that we often observe (i.e., $n = 12$ and 14 are often larger than $n = 11$, 13, and 15).[21]

Figure 4 shows two model structures for $[16(\text{Ser})+2\text{H}]^{2+}$ that could be produced from combining compact $[8(\text{Ser})+\text{H}]^+$ model structures that have cross sections that are in agreement with experiment (for $[8(\text{Ser})+\text{H}]^+$). Structure 4a is formed by combining the octamer units along the longest face (11.2 × 7.2 Å) of the octamer unit, and structure 4b is formed by bringing the units together at the smallest face (6.7 × 7.2 Å). While the systems are tightly packed, the calculated cross sections of 367 and 389 Å^2, for structures 4a and 4b, respectively, are much larger than the experimental value of 294.0 observed for the $[16(\text{Ser})+2\text{H}]^{2+}$ cluster. Comparisons of assemblies of the larger $[24(\text{Ser})+3\text{H}]^{3+}$ and $[32(\text{Ser})+4\text{H}]^{4+}$ clusters from the octamer subunits are also much larger than the corresponding experimental values. Molecular dynamics simulations of these larger systems do produce low-energy geometries that are in agreement with experiment; however, the structures are substantially more spherical in nature. Although we cannot rule out the possibility of symmetric elements within this cluster, there is no strong evidence for such structure. Overall, the system appears to maximize zwitterionic contacts between monomer units while forming clusters that have roughly spherical geometries.

A question that arises in the assembly of large biomolecular clusters is the degree to which the structures of isolated clusters resemble structures in condensed phases (i.e., solution and crystals). Previous studies have shown that in some systems, relatively nonspecific aggregates are formed;[22] in other systems (e.g., complementary oligonucleotide sequences and enzyme−substrate systems), specific geometries appear to be favored.[23] The observation that larger clusters ($n = 16$, 24, and 32) appear to be assembled from octamer building blocks but do not appear to adopt a long range order that is induced by the octamer unit is interesting; however, several interpretations are possible. An interesting interpretation is that the gas-phase structures that we observe resemble those that exist in solution. In this case, when two octamer units coalesce, it appears that the larger cluster that is formed rapidly rearranges to generate a more spherical geometry. This would suggest that the structures of small serine clusters reconstruct before assuming the structure of the bulk crystal. It is also possible that the cluster geometries that we have sampled reflect the structures of ions in the gas phase. In this case, it would not be surprising that large clusters have geometries that cannot be represented as assemblies of $[8(\text{Ser})+\text{H}]^+$ clusters. We are currently examining a number of related systems in order to address these issues in more detail.[24]

Summary and Conclusions

Recent proposals of structures for the magic number serine cluster $[8(\text{Ser})+\text{H}]^+$ have led us to investigate the configuration directly using ion mobility and molecular modeling techniques. Our results indicate that $[8(\text{Ser})+\text{H}]^+$ is composed of seven zwitterionic serine units and a single serine that is protonated at the amino terminus. The interactions between these units leads to tightly packed structures with distorted blocklike geometries having dimensions of approximately 11.2 × 6.7 × 7.2 Å. Magic numbers in the mass spectrum at $n = 16$ and $n = 24$ suggest that the serine octamer is a building block in the assembly of larger clusters. The geometries of these larger clusters are roughly spherical and do not appear to resemble the distorted blocklike structures found for $[8(\text{Ser})+\text{H}]^+$. Further studies are underway to investigate the importance of chirality in these systems.

Acknowledgment. The authors gratefully acknowledge financial support from the National Institutes of Health (Grant No. 1R01GM59145-01 and 55647-03) and National Science Foundation (CHE-0078737).

References and Notes

(1) See, for example: Vekey, K.; Czira, G. *Anal. Chem.* **1997**, *69*, 1700. Ramirez, J.; He, F.; Lebrilla, C. B. *J. Am. Chem. Soc.* **1998**, *120*, 7387. Yao, Z.; Wan, T. S. M.; Kwong, K.; Che, C. *Chem. Commun.* **1999**, *20*, 2119. Tao, W. A.; Zhang, D. X.; Nikolaev, E. N.; Cooks, R. G. *J. Am. Chem. Soc.* **2000**, *122*, 10 598.

(2) Hodyss, R.; Julian, R. R.; Beauchamp, J. L., submitted for publication.

(3) Zhang, D.; Koch, K. J.; Tao, A.; Cooks, R. G. Proceedings of the 48th ASMS Conference on Mass Spectrometry and Allied Topics, 2000, p 1361−1362.

(4) The term magic number is used to indicate a cluster size that appears to exhibit unusual stability. See ref 8 for details.

(5) Since the submission of our paper, we have learned of additional studies by Cooks and co-workers in which a cubelike geometry is proposed. [Cooks, R. G.; Zhang, D.; Koch, K. J.; Gozzo, F. C.; Eberlin, M. N., personal communication, May 2001.]

(6) Hagen, D. F. *Anal. Chem.* **1979**, *51*, 870. Hill, H. H.; Siems, W. F.; St. Louis, R. H.; McMinn, D. G.; *Anal. Chem.* **1990**, *62*, 1201A.

(7) For recent reviews of ion mobility studies of biomolecules, see: Clemmer, D. E.; Jarrold, M. F. *J. Mass Spectrom.* **1997**, *32*, 577. Hoaglund Hyzer, C. S.; Counterman, A. E.; Clemmer, D. E. *Chem. Rev.* **1999**, *99*, 3037.

(8) For recent reviews, see for example: Morse, M. D. *Chem. Rev.* **1986**, *86*, 1049. Jarrold, M. F. *J. Phys. Chem.* **1995**, *99*, 11. Castleman, A. W., Jr.; Bowen, K. H., Jr. *J. Phys. Chem.* **1996**, *100*, 12 911. Bacic, Z.; Miller, R. E. *J. Phys. Chem.* **1996**, *100*, 12 945.

(9) Fenn, J. B.; Mann, M.; Meng, C. K.; Wong, S. F.; Whitehouse, C. M. *Science* **1989**, *246*, 64.

(10) Hoaglund, C. S.; Valentine, S. J.; Sporleder, C. R.; Reilly, J. P.; Clemmer, D. E. *Anal. Chem.* **1998**, *70*, 2236. Henderson, S. C.; Valentine, S. J.; Counterman, A. E.; Clemmer, D. E. *Anal. Chem.* **1999**, *71*, 291.

(11) Mason, E. A.; McDaniel, E. W. *Transport Properties of Ions in Gases*. Wiley: New York 1988.

(12) von Helden, G.; Hsu, M.-T.; Kemper, P. R.; Bowers, M. T. *J. Chem. Phys.* **1991**, *95*, 3835. Jarrold, M. F.; Constant, V. A. *Phys. Rev. Lett.* **1991**, *67*, 2994. Clemmer, D. E.; Hudgins, R. R.; Jarrold, M. F. *J. Am. Chem.* Soc. **1995**, *117*, 10 141.

(13) InsightII, Biosym/MSI: San Diego, CA, 1995.

(14) Mesleh, M. F.; Hunter, J. M.; Shvartsburg, A. A.; Schatz, G. C.; Jarrold, M. F. *J. Phys. Chem.* **1996**, *100*, 16 082.

(15) Lee, S.; Wyttenbach, T.; von Helden, G.; Bowers, M. T. *J. Am. Chem. Soc.* **1995**, *117*, 10 159.

(16) Shvartsburg, A. A.; Jarrold, M. F. *Chem. Phys. Lett.* **1996**, *261*, 86.

(17) Valentine, S. J.; Counterman, A. E.; Hoaglund, C. S.; Reilly, J. P.; Clemmer, D. E. *J. Am. Soc. Mass Spectrom.* **1998**, *9*, 1213.

(18) We cannot rule out the possibility that there is a distribution of configurations that rapidly interconvert. In this case, our measurement would reflect the average cross section associated with the distribution. Although such behavior may be the case for some compact geometries, we rule out the possibility that clusters with large cross sections (factors of 1.1 or greater than experiment) based on the observation that the calculated energies of these geometries are usually greater than the lowest energy structures by more than ~15 kcal•mol^{-1}. See text for a detailed discussion.

(19) Wyttenbach, T.; von Helden, G.; Bowers, M. T. *J. Am. Chem. Soc.* **1996**, *118*, 8355. Hoaglund, C. S.; Liu, Y.; Pagel, M.; Ellington, A. D.; Clemmer, D. E. *J. Am. Chem. Soc.* **1997**, *119*, 9051. Counterman, A. E.; Clemmer, D. E., *J. Am. Chem. Soc.* **1999**, *121*, 4031.

(20) Average dimensions were determined from measurements of the lowest energy structures found from each of five replicate molecular dynamics simulations performed at 300 K for 0.25 ns. The lowest energy structures from each simulation are typical representatives of the geometries observed after ~0.1 ns in each simulation. Uncertainties are taken to be one standard deviation about the mean value.

(21) The relative intensities of the $[n(\mathrm{Ser})+2\mathrm{H}]^{2+}$ ($n = 8$ to 16) clusters depend on the experimental conditions. One interesting observation is that the $[10(\mathrm{Ser})+2\mathrm{H}]^{2+}$ ion is virtually absent in all of the datasets that we have recorded. Although we do not understand this behavior entirely, it appears that this cluster size is much less stable than the range of other $[n(\mathrm{Ser})+2\mathrm{H}]^{2+}$ ions that are observed.

(22) Meng, C. K.; Fenn, J. B. *Org. Mass Spectrom.* **1991**, *26*, 542. Busman, M.; Knapp, D. R.; Schey, K. L. *Rapid Comm. Mass Spectrom.* **1994**, *8*, 211. Thomson, B. A. *J. Am. Soc. Mass Spectrom.* **1997**, *8*, 1053. Counterman, A. E.; Valentine, S. J.; Srebalus, C. A.; Henderson, S. C.; Hoaglund, C. S.; Clemmer, D. E. *J. Am. Soc. Mass Spectrom.* **1998**, *9*, 743.

(23) Ganem, B.; Li, Y.-T.; Henion, J. D. *J. Am. Chem. Soc.* **1991**, *113*, 6294. Katta, V.; Chait, B. T. *J. Am. Chem. Soc.* **1991**, *113*, 8534. Baca, M.; Kent, S. B. H. *J. Am. Chem. Soc.* **1992**, *114*, 3992. Smith, R. D.; Light-Wahl, K. J., Winger, B. E.; Loo, J. A. *Org. Mass Spectrom.* **1992**, *27*, 811. Schnier, P. D.; Klassen, J. S.; Stritmatter, E. E.; Williams, E. R. *J. Am. Chem. Soc.* **1998**, *120*, 9605.

(24) Counterman, A. E.; Clemmer, D. E., work in progress.

(25) Benedetti, S.; Pedone, C.; Sirigu, A. *Cryst. Struct. Comm.* **1972**, *1*, 35. Kistenmacher, T. J.; Rand, G. A.; Marsh, R. E. *Acta Crystallogr. B* **1974**, *30*, 2573.